

Gum Arabic microencapsulated *Spondia mombin* particles induced delayed modulatory potential on testosterone-induced benign prostatic hyperplasiaIgharo Aiseosa Kingsley^{*1}, Nnamani Didacus², Adedokun Oluwasegun³, Kehinde Ibrahim⁴¹Department of Pharmaceutics and Pharmaceutical Technology, Igbiniedion University, Edo State, Nigeria²Department of Pharmaceutics and Pharmaceutical Technology, Igbiniedion University, Edo State, Nigeria,³CBIOS – Universidade Lusofona's Research Center for Bioscience and Health Technologies, Lisbon, Portugal⁴Department of Pharmaceutical Chemistry, College of Pharmacy, Afe Babalola University, NigeriaSubmitted: 23rd Sept., 2024; Accepted: 29th Sept., 2024; Published online: 31st October, 2024DOI: <https://doi.org/10.54117/jcbr.v4i5.4>*Corresponding Author: Igharo Aiseosa Kingsley; aiseosaigharo@gmail.com**Abstract**

Spondia mombin stems are traditionally used for managing benign prostatic hyperplasia (BPH). This study examines the impact of microencapsulation on *S. mombin*'s anti-BPH properties, comparing the crude and encapsulated extracts. Microencapsulated particles of *S. mombin* (S-Mp) were prepared using acacia gum and characterized through Scanning Electron Microscopy (SEM), Energy Dispersive X-ray (EDX), Fourier Transform Infrared Spectroscopy (FTIR), micromeritic analysis, and dissolution studies. The anti-BPH activity of S-Mp, blank particles (B-Mp), and crude extracts was evaluated in vivo by measuring prostate-specific antigen (PSA), serum testosterone, and prostate index (PI) in male rats. SEM analysis showed larger particle sizes in S-Mp (50–80 μm) compared to B-Mp (>50) which may indicate the addition of active drug in the

blank microspheres or due to other cohesive forces affecting particle size distribution, drug agglomeration. EDX revealed the presence of oxygen, sodium, carbon, and sulfur in both S-Mp and B-Mp, with significant compositional differences. FTIR analysis identified additional peaks in S-Mp, suggesting interactions with acacia gum. Micromeritic analysis demonstrated improved flow properties for S-Mp, with an angle of repose of 27.9°, compressibility index of 6.06%, and Hausner's ratio of 1.06, indicating better handling potential. Dissolution studies revealed that S-Mp had significantly higher absorbance values compared to B-Mp at all time points, indicating enhanced dissolution rates. The absorbance of S-Mp steadily increased from 0.9085 at 5 minutes to 1.2600 at 60 minutes, while B-Mp showed lower and relatively constant values throughout. In vivo, the crude extract demonstrated dose-dependent

PSA reduction, peaking at 400 mg/kg, while S-Mp showed maximum reduction at 100 mg/kg, with diminished effects at higher doses. Encapsulation delayed release and reduced overall efficacy, as reflected in the dissolution data. Serum testosterone levels also decreased significantly upon encapsulation. *S. mombin* exhibits notable anti-BPH activity, but microencapsulation with acacia gum reduces efficacy due to delayed release, despite improved dissolution rates.

Keywords: *Spondia mombin*, microencapsulation, pharmaceuticals, benign prostatic hyperplasia, acacia gum, dissolution, prostate-specific antigen.

Introduction

Benign Prostatic Hyperplasia (BPH) is a benign growth of the prostate gland that typically affects older men and causes problems related to urination. (Kim et al., 2016). The prevalence of BPH rises with age globally, impacting more than 50% of men who are 50 years of age or older (Lee et al., 2017; Xiong et al., 2020). Alpha-blockers and 5-alpha reductase inhibitors are two common treatments for BPH in conventional medicine (Kim et al., 2018; Lepor, 2016); nevertheless, adverse effects and insufficient effectiveness have led to the investigation of complementary and

alternative medicine. Drug delivery must overcome biological barriers, minimize adverse effects, and distribute therapeutic chemicals to precise locations in the body in a targeted and regulated manner, among other difficulties (Adepu & Ramakrishna, 2021). These issues are addressed by microencapsulation, which encapsulates medications in tiny particles that are frequently composed of biocompatible materials (Singh et al., 2010). These capsules range in size from 0.001 mm to 7 mm, and depending on their intended use, they release their contents at a predetermined time (Rani & Goel, 2021). This method improves the drug's stability, protects it, and permits a prolonged release (Singh et al., 2010). Furthermore, medications can be delivered to certain tissues or cells through the use of microencapsulation, increasing their therapeutic efficacy and lowering systemic toxicity (Lam & Gambari, 2014; Lengyel et al., 2019). The precise control over release kinetics and the ability to protect sensitive drugs from degradation make microencapsulation a valuable tool for overcoming the complexities associated with drug delivery (Lopez-Mendez et al., 2021; H. Singh, 2023; Singh et al., 2010). The capacity to precisely manage release kinetics and shield delicate medications from deterioration makes

microencapsulation an invaluable tool for navigating the challenges of drug delivery (Sarode et al., 2024).

Spondia mombin is one of the herbal remedies for BPH control that has been studied (Iwu et al., 2022). It may have anti-inflammatory and antioxidant qualities (Adeniran et al., 2021; Asante Ampadu et al., 2022; Nworu et al., 2011; Ogunro et al., 2023). *S. mombin*, a member of the Anacardiaceae family, is a plant species that grows in Nigeria (Adeniran et al., 2021). The fruit is known by several names in the region: Iyeye or Yeye in Yoruba, Ngulungwu in Igbo, Ughighen in Urhobo, and Isada in Hausa (Aiyeloja & Bello, 2006; Aromolaran & Badejo, 2014). Leprosy, severe cough, diarrhoea, dysentery, dyspepsia, gastralgia, colic, constipation, haemorrhoids, gonorrhoea, leucorrhoea, dystocia, postpartum haemorrhage, inflammation have all been treated locally with this plant (Iwu et al., 2022; Ogunro et al., 2023; Osuntokun, 2018, 2019, 2019).

The objectives of this study are to produce and analyze microencapsulated *S. mombin* particles, compare the anti-BPH screening efficaciousness of *S. mombin* extract and microparticles, and experimentally validate the use of *S. mombin* in the treatment of BPH.

Materials and methods

Plant collection

The stem bark of *S. mombin* was obtained from the Federal Research Institute of Nigeria, located in Ibadan, Oyo State. This collection involved a systematic and careful harvesting process to ensure the quality and authenticity of the plant material (Alamgir & Alamgir, 2017). A voucher specimen was deposited at the herbarium section of the research institute

Animals

Male Wistar Rats weighing around 140 - 211.2 g were sourced from the Animal House at the University of Benin, Edo State. They were fed with a standard rat pelleted diet (Bendel Feeds and Flower Mill, Edo state, Nigeria) and water ad-libitum and maintained under hygienic standard laboratory conditions (temperature, 25 °C; photoperiod, 12 h of natural light and 12 h of dark).

Extraction

The stem bark of *S. mombin* was rinsed in water and air-dried by spreading it on a clean sack devoid of sand for 2 weeks. A laboratory milling machine was used to reduce the dried plant material to coarse powder. The powdered plant material was extracted with methanol using a Soxhlet apparatus. The resulting extract was in turn

concentrated to dryness using a water bath (HH-S Water Bath; Searchtech Instruments) at a temperature of 60 °C.

Preparation and characterization of *s. mombin* microcapsules

Microencapsulation of *S. mombin*

In a modified coacervation process (Thilagavathi et al., 2007), 40 g of acacia was gradually made up to 400 mL with hot water with stirred for 2 minutes on a hot plate magnetic stirrer (Model TK23, Kartell, Italy). The dispersion was allowed to stand and swell for 1 hr. A mixture of 40 g *S. mombin* and 40 mL sodium sulphate solution (anti-aggregating agent) was made and added to the swollen dispersion by stirring on the hot plate for 2 minutes. An 80 ml absolute ethanol (for coacervation) was added drop-wise at 1 mL/min from a height of 5 cm. The coarse dispersion was kept in a Pharmaceutical Lyophilizer Freezer Dryer, (Harvest Right 110V Seven Tray Freezer Dryer with Stainless Steel Vacuum Pump, Model; SKU: HR-MEDPHRM) at - 18 C for 12 hr. The preparation was removed from the freezer, pulverized to granule sizes, and heated for 1 min at 140 C in an open Bunsen burner flame to dry. The heated material was allowed to cool to dryness. The dried material was pulverized, passed through a 1.7 mm stainless steel sieve, packed, labelled, and stored for further analysis.

Characterization of blank and SM-Microparticles

Fourier Transform Infrared Spectroscopy of Microencapsulated *Spondia mombin* L. extract and blank

Fourier-transform infrared (FTIR) analysis was used to identify the functional groups in secondary metabolite compounds from the *S. mombin* extract, and microencapsulated products (Sangeetha et al., 2019). The FTIR spectra for all the samples were obtained using a Jasco FT-IR 4000/6000 series spectrometer, Jasco Oklahoma, USA. A 5 mg sample was mixed with solid potassium bromide (KBr) powder after which the transmittance was recorded at wavelengths of 700–4000 cm^{-1} (George et al., 2021).

Scanning electron microscopy (SEM) of Microencapsulated *Spondia mombin* L. extract and blank

Scanning electron microscopy Analysis of the morphology of the *S. mombin* and control microspheres was performed using a JEOL JSM-65 10LV type scanning electron microscope (SEM). The microcapsules were coated with platinum. Resolution high vacuum (HV) mode was 3.0 nm (30 kV), low vacuum (LV) mode was 4.0 nm (30 kV), and accelerating voltage ranged from 0.5 kV to 30 kV (Jayanudin et al., 2019).

Energy Dispersive X-ray (EDX) of Microencapsulated *Spondia mombin* L. extract and blank

The energy dispersive X-ray microanalytical studies of the *S. mombin* and control microspheres were carried out using the same equipment for SEM (JEOL JSM-65 10LV type) provided with EDAX DX-4 eDXi System, version 2.11. Between 0 and 20 keV, EDAX spectra were obtained using an X-ray detector that had an extremely small window. The spectrum was collected over 120 seconds (Liu et al., 2007).

Micromeritic Evaluation of Microencapsulated Extract and Control Angle of repose

The angle of repose, α , was determined by measuring the height of the cone of the powder and the width occupied by the powder when poured by using the equation below (Taylor & Aulton, 2021).

$$\tan(\alpha) = \frac{\text{height}}{0.5 \times \text{base}}$$

Compressibility Index and Hausner ratio

The compressibility index and the Hausner ratio were determined by measuring the apparent unsettled volume, V_o , and the final tapped volume, V_f , of the powder after mechanically tapping a graduated measuring cylinder containing the powder no further volume changes occurred. The weight of the powder was also determined using the

weight by difference method and was used to calculate the Bulk density and tapped density or vessel containing the powder sample

The formula to obtain the Bulk and Tapped densities is given below.

$$\text{Bulk Density } (\rho_o) = \frac{\text{Weight of Powder}}{V_o}$$

$$\text{Tapped Density } (\rho_f) = \frac{\text{Weight of Powder}}{V_f}$$

The compressibility index and the Hausner ratio are calculated by the following Equations

$$\text{Compressibility Index} = 100 \times \frac{\rho_f - \rho_o}{\rho_f}$$

$$\text{Hausner Ratio} = \frac{\rho_f}{\rho_o}$$

In vivo anti-bph effect of crude and microencapsulated *s. mombin* particles

Induction of BPH using testosterone

In inducing BPH in the animals (Li et al., 2018), 25 mg/kg of testosterone propionate injection (Sustanon 250 mg/mL) dissolved in olive oil was administered subcutaneously to all Wister rats (n = 24) except the normal control group (n=3) for 28 consecutive days after 7 days of acclimatization of the entire animals.

Biological evaluation of anti-BPH effect

Twenty seven male Wister rats were grouped equally into nine (9) different categories, namely; The negative controls (NEC- distilled water), positive controls (PC - 100 mg/kg Finasteride), normal controls (NOC; no induction of BPH to this group) while groups S1, S2 and S3 (*S. mombin* - 100, 200 and 400 mg/kg, and groups ES1, ES2 and ES3 (microencapsulated *S. mombin* - 100, 200, and 400 mg/kg body of microencapsulated *S. mombin*) making three rats per group. The oral administrations of the samples were done for each group for 28 consecutive days.

Preparation of samples for biological analysis

On the last day of administration, the final weight of the animals was taken, and the animals were then anaesthetized using chloroform and dissected. The prostate was carefully removed surgically using forceps and scissors, the sample was immediately transferred into a normal saline bath in a sample bottle for homogenization and further analysis (Smith & Xu, 2012). Untreated animals showed a significant increase in prostate size compared to the groups that received treatment.

Additionally, the blood of each animal was collected via cardiac puncture using a 5 mL sterile syringe into each labelled clean

EDTA (to collect plasma) and non-coagulant (plain; to collect serum) sample bottles and frozen at 4°C (Parasuraman et al., 2010)

Determination of serum PSA and serum percentage prostate health index (PHI)

The homogenized prostate glands were stored at 4°C before centrifugation for 20 min at 1000×g at 4°C. The supernatant was collected to carry out the assay. The blood collection tubes prepared were disposable and free from endotoxins. The fully automated immunoassay device Access® (Beckman Coulter, Brea, California) at Ekiti State University Teaching Hospital was used for the *in vitro* quantitative determination of PSA concentrations and Prostate Health Index in the serum of the Wistar rats

Determination of Serum Testosterone

The amount of serum testosterone (ng/mL) was assayed quantitatively using testosterone coated-tube radioimmunoassay kits (Siemens Healthcare Diagnostics, Inc., Washington D.C.), which had a lower limit of detection of 0.04 ng/mL

Dissolution study of the blank and sm-microparticles

A calibrated dissolution apparatus (USP II) was used with the paddle at 75 rpm and bath temperature was maintained at $37 \pm 0.5^\circ\text{C}$. 900mL freshly prepared 0.1 N HCl solution was used as the dissolution medium.

Dissolution samples were collected at 5, 10, 15, 30, 45, and 60 min for the 0.5g blank sample (B-Mp) and duplicates of 0.5g Microencapsulated *Spondia mombin* samples (S-Mp 1 and S-Mp 2) and replaced with an equal volume of the fresh medium to maintain a constant total volume. At each time point, a 5 mL sample was removed from each vessel and filtered into labelled glass tubes, diluted and analysed by UV at wavelength 300 nm.

Data analysis

One Way ANOVA was done to compare the means of different groups as well as a Dunnett's test to analyze differences among different means and the interaction between the variables using GraphPad Prism 7 Software Package. Data was presented as mean \pm SEM of three replicates (n=3 per animal group) and Differences at $p \leq 0.05$ were considered statistically significant.

Results

Result of ftir analysis of blank and microencapsulated particles of *S. mombin*

The FTIR analysis of the blank (B-Mp) and microencapsulated particles of the plant extract (S-Mp) showed several peak similarities in terms of wavenumber and intensity. Peaks with wave numbers 2929.7 and 2117.1 were observed with blank and microencapsulated particles of *S. mombin* spectra. However, despite the similarities in these wavenumbers, the difference in intensities was observed ((2929.7 - 80.111 (B-Mp) vs 70.984 (S-Mp) and 2117.1 - 93.735 (B-Mp) vs 96.499 (S-Mp)) indicating that both *S. mombin* extract (core) and acacia (matrix) were mixed. Microencapsulated particles were formed, hence the changing intensity. Also, similar wavenumbers in both indicate that the matrix (acacia) is present in the *S. mombin* microencapsulated formed, as shown in Figure 5

However, there were some differences in peaks which showed the peculiarity of the blank (B-Mp) and *S. mombin* microencapsulated particles (S-Mp). Peak wavenumber 838.7 with an intensity of 68.524 was noted in the B-Mp but not in S-Mp particles, which might be a distinct characteristic of acacia gum. In addition, peak wavenumbers 1256.1, 1226.3,

and 1599.0 with intensities of 80.262, 80.542, and 73.034 were not present in S-Mp particles.

In addition, peak wavenumbers of 1110.7, 1449.9, and 1364.2 with intensities of

42.699, 71.605, and 68.665, respectively were also peculiar to S-Mp particles but absent in the B-Mp particles, these reflect the composition of the active ingredient.

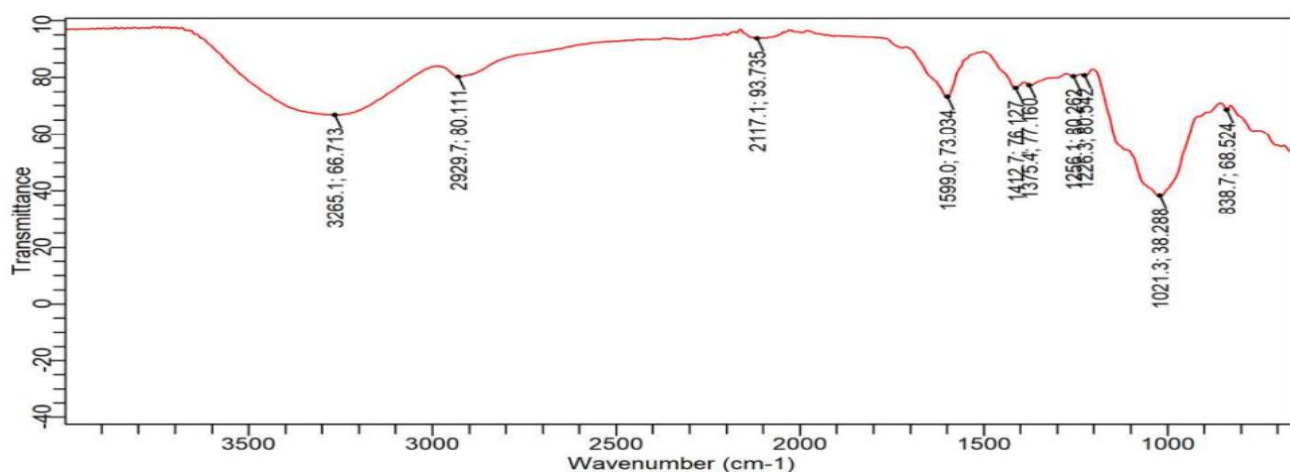


Figure 5: FTIR Spectroscopy of the blank microparticles (B-Mp).

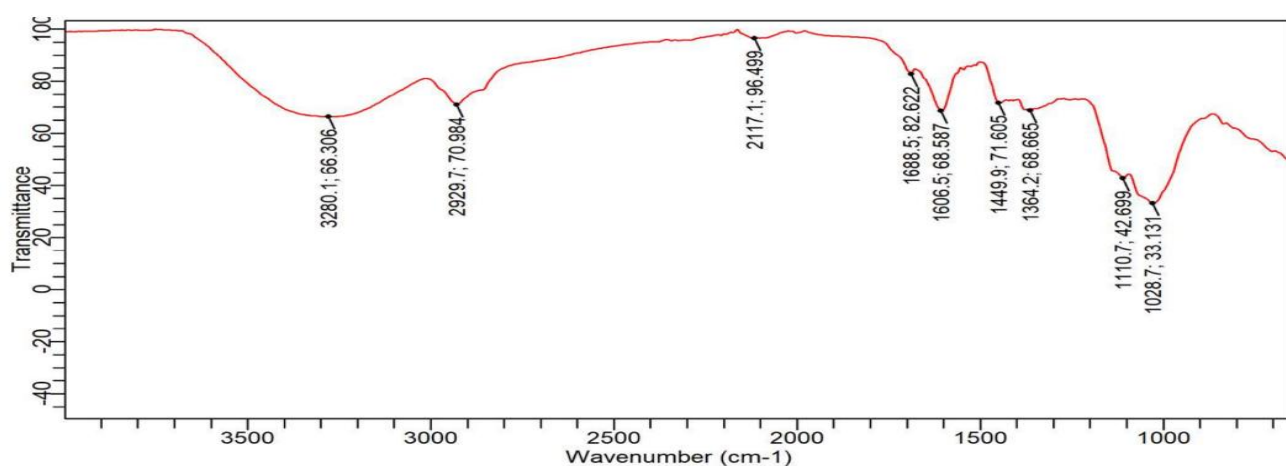


Figure 6: FTIR Spectroscopy of microencapsulated *S. mombin* (S-Mp) particles.

Scanning electron microscopy (sem) and edx microanalysis of microencapsulated extract and blank

A backscattered electron detector (BSD) that detects elastically scattered electrons was used in the SEM. A comparison of the SEM of both B-Mp and S-Mp at a magnification of $\times 1500$ (Figures 7a and 7b) showed that the S-Mp particle size is bigger with a diameter greater than 50 microns. This may either be due to which may indicate the addition of active drug in the blank microspheres or due to other cohesive forces affecting particle size distribution. The

microparticles of the B-Mp were smooth and sharp-edged whereas S-Mp particles were more granular.

A comparison of the SEM of both the B-Mp and S-Mp at a magnification of $\times 1000$ (Figures 8a and 8b) shows that the particle size of the S-Mp particles has a diameter of around 80 microns. This is not true for the B-Mp which has less than 50 microns in width. The observed microparticles at this magnification of the blank are also smooth and sharp-edged whereas S-Mp is more granular.

In addition, a comparison of the SEM of both the B-Mp and S-Mp at a magnification of $\times 600$ (Figures 9a and 9b) shows that S-Mp has a width diameter of bigger than 100 microns. The B-Mp still has width sizes which have less than 50 microns. Similar to the $\times 1000$ and $\times 1500$ magnifications, the observed microparticles at this magnification of the blank is also smooth and sharp-edged whereas S-Mp maintains its more granular texture. Similar to the $1000\times$ and $\times 1500$ magnifications, the particle sizes of S-Mp are observed to be oval in shape and its particle size distribution has more fines or smaller particles below 25microns, as compared to the blank, some particles of the microencapsulated *Spondia mombin* and a majority of the blank were observed to have irregular shapes with sharp edges.

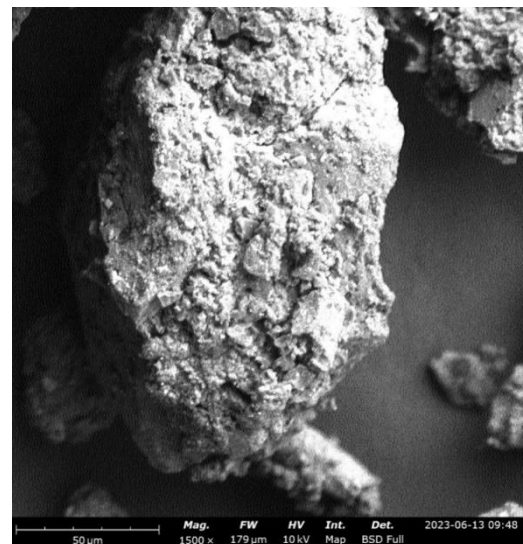
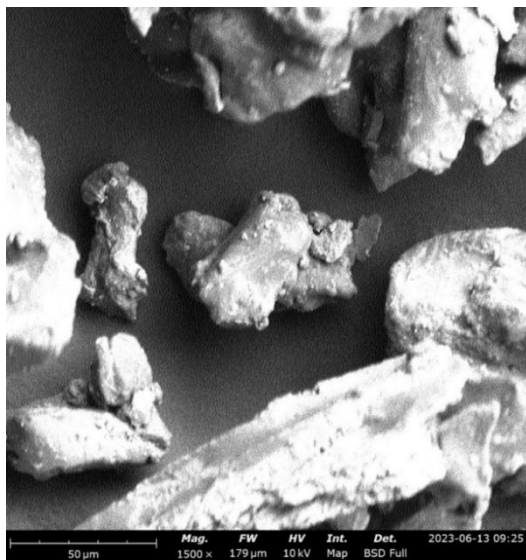


Figure 7a: SEM of B-Mp at $\times 1500$

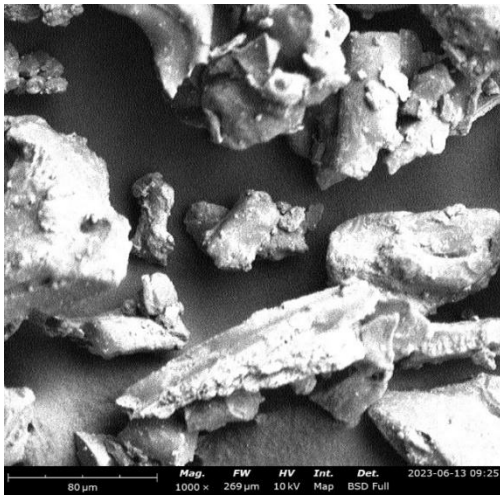


Figure 7b: SEM of S-Mp at $\times 1500$

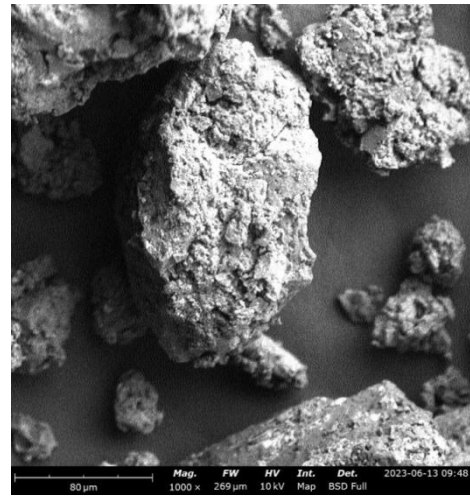


Figure 8a: SEM of B-Mp at $\times 1000$

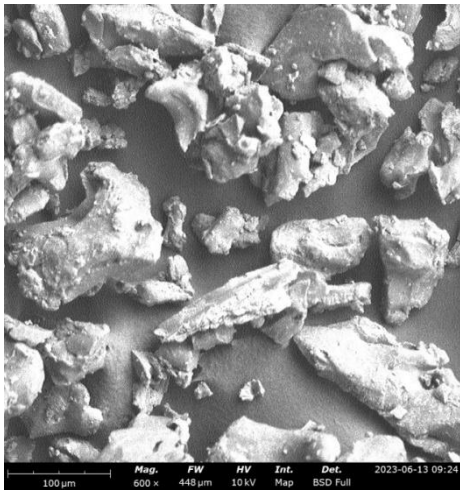


Figure 8b: SEM of S-Mp at $\times 1000$

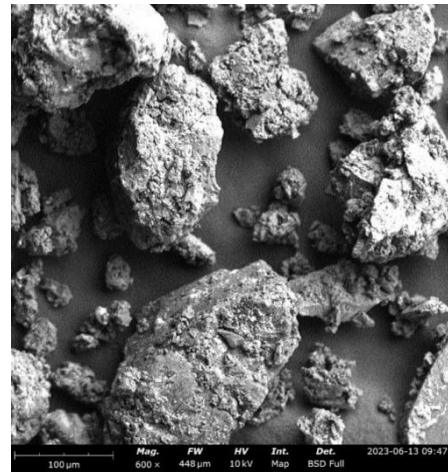


Figure 9a: SEM of B-Mp at $\times 600$

Figure 9b: SEM of S-Mp at $\times 600$

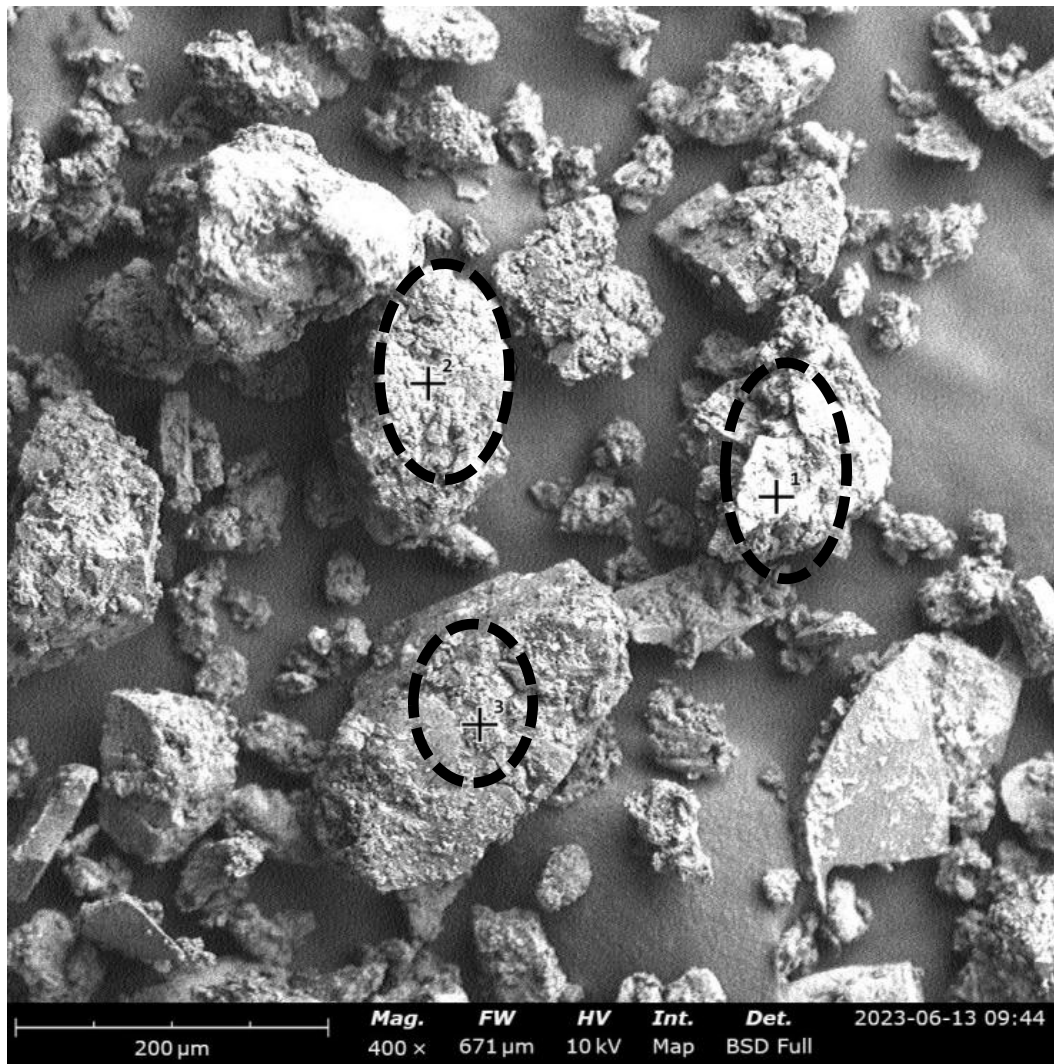


Figure 10: EDX microanalysis of S-Mp showing the 3 identified spots where EDX analysis was done

A backscattered electron detector was also used in the EDX microanalysis at $\times 400$ magnification. The elemental constituents in the B-Mp and S-Mp particles were determined. However, three spots were identified and tested for the elements they contained at those spots. The spots were numbered Spot 1, Spot 2 and Spot 3 and they were compared (Figure 10, Table 4 - 6), prevalent elements that can be observed in EDX analysis were Oxygen, Sodium, Carbon and Sulphur in Spot 1, Oxygen, Calcium, and Sulphur in Spot 2 and Oxygen, Sodium, and Carbon in Spot 3. In all three spots, Oxygen presented with the most atomic and weight concentrations at 66.09% and 58.70 % which is similar to the values found in S-Mp particles at 63.60% and 56.18% in Spot 1, 75.25% and 57.37% in Spot 2, and 67.23% and 63.98% in Spot 3 which is also remarkably similar to the values found in S-Mp particles at 66.50% and 63.47% in Spot 3.

Table 4: Constituent elements in Spot 1 of the EDX analysis of S-Mp particles.

Element Number	Element Symbol	Element Name	Atomic Conc.	Weight Conc.
8	O	Oxygen	63.60	56.18
11	Na	Sodium	21.57	27.38
6	C	Carbon	8.86	5.87
16	S	Sulphur	5.97	10.57

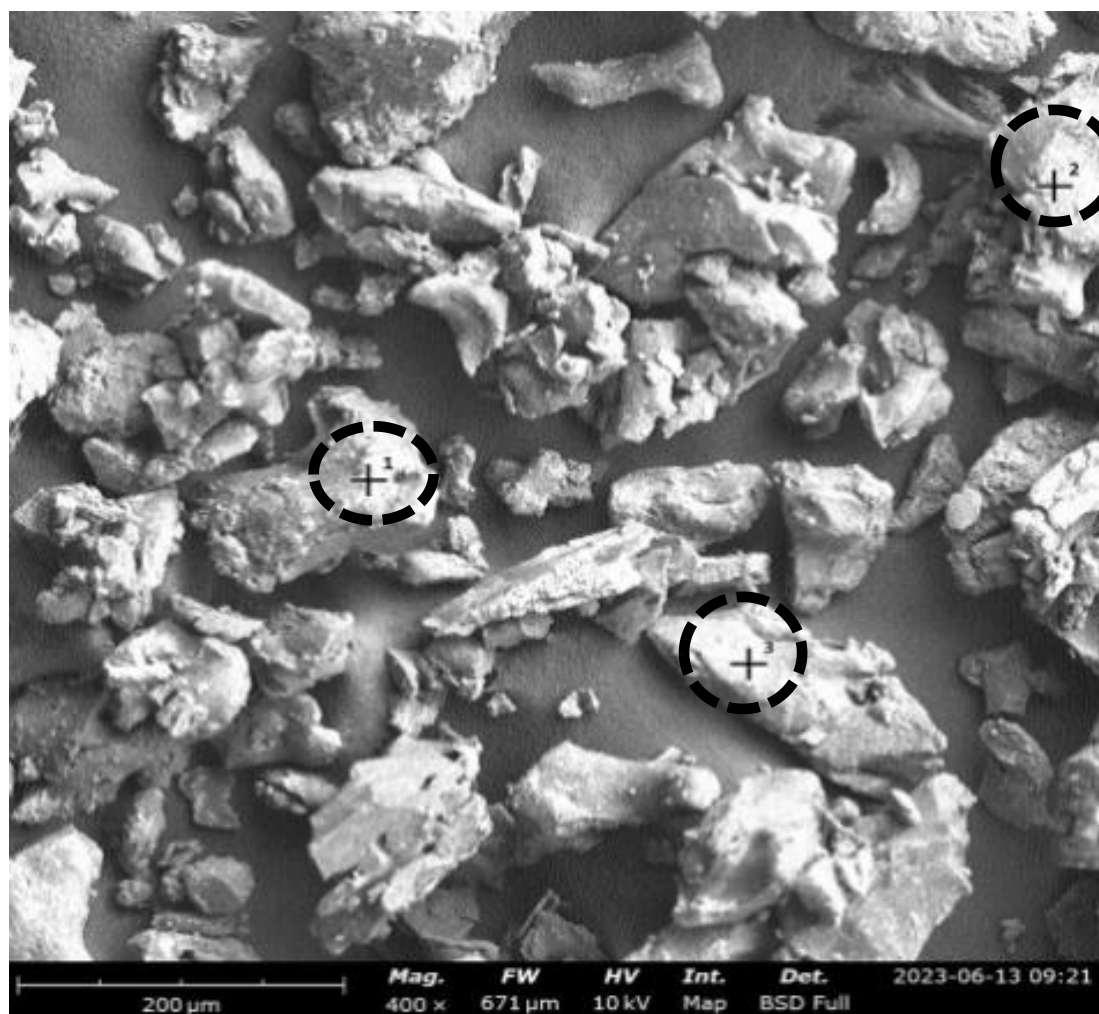
Table 5: Constituent elements in Spot 2 of the EDX analysis of S-Mp particles.

Element Number	Element Symbol	Element Name	Atomic Conc.	Weight Conc.
8	O	Oxygen	52.06	39.49
11	Na	Sodium	28.79	31.38
16	S	Sulfur	19.16	29.13

Table 6: Constituent elements in Spot 3 of the EDX analysis of S-Mp particles.

Element Number	Element Symbol	Element Name	Atomic Conc.	Weight Conc.
8	O	Oxygen	66.50	63.47
11	Na	Sodium	19.14	26.25
6	C	Carbon	14.36	10.29

In contrast to S-Mp particles, sodium was only found in two spots, and a different element calcium was also observed, this could be a random occurrence as there may be a large number of elements that may be present in trace amounts throughout the analysed samples, but in all cases, oxygen was most predominant in the microencapsulated samples.

**Figure 11: EDX microanalysis of B-Mp showing the 3 identified spots where EDX analysis was done**

Element Number	Element Symbol	Element Name	Atomic Conc.	Weight Conc.
8	O	Oxygen	66.09	58.70
11	Na	Sodium	18.17	23.19
6	C	Carbon	8.89	5.93
16	S	Sulphur	6.84	12.18

Table 7: Constituent elements in Spot 1 of the EDX analysis of B-Mp**Table 8: Constituent elements in Spot 2 of the EDX analysis of B-Mp**

Element Number	Element Symbol	Element Name	Atomic Conc.	Weight Conc.
8	O	Oxygen	75.25	57.37
20	Ca	Calcium	12.60	24.06
16	S	Sulphur	12.15	18.57

Table 9: Constituent elements in Spot 3 of the EDX analysis of B-Mp

Element Number	Element Symbol	Element Name	Atomic Conc.	Weight Conc.
8	O	Oxygen	67.23	63.98
11	Na	Sodium	19.32	26.42
6	C	Carbon	13.44	9.60

Result from micromeritic evaluation of microencapsulated extract and control

The flow and compressibility characteristics of two different powder samples, B-Mp and S-Mp, were evaluated using various parameters, including bulk and tapped densities, compressibility index, and Hausner's ratio (Table 10). The angle of repose, which is a measure of flowability, was found to be 32.00° for B-Mp and 27.90° for S-Mp, indicating that S-Mp has slightly better flow properties compared to B-Mp.

B-Mp exhibited a bulk density of 0.71 g/mL, while S-Mp had a higher bulk density of 0.93 g/mL. Similarly, the tapped density for B-Mp was 0.81 g/mL, whereas S-Mp showed a higher tapped density of 0.99 g/mL. These results suggest that S-Mp particles are more closely packed than B-Mp particles when subjected to tapping.

The compressibility index, which reflects the powder's ability to decrease in volume under pressure, was calculated to be 12.35% for B-Mp and 6.06% for S-Mp. Lower compressibility indices generally indicate better flowability, with S-Mp demonstrating superior flow

properties compared to B-Mp. Hausner's ratio, another measure of flowability, further supports this finding, with values of 1.14 for B-Mp and 1.06 for S-Mp. Typically, a Hausner's ratio close to 1.00 suggests good flowability; thus, S-Mp exhibits better flow properties than B-Mp.

Table 10 Micromeritic Results of Microencapsulated Extract and Control

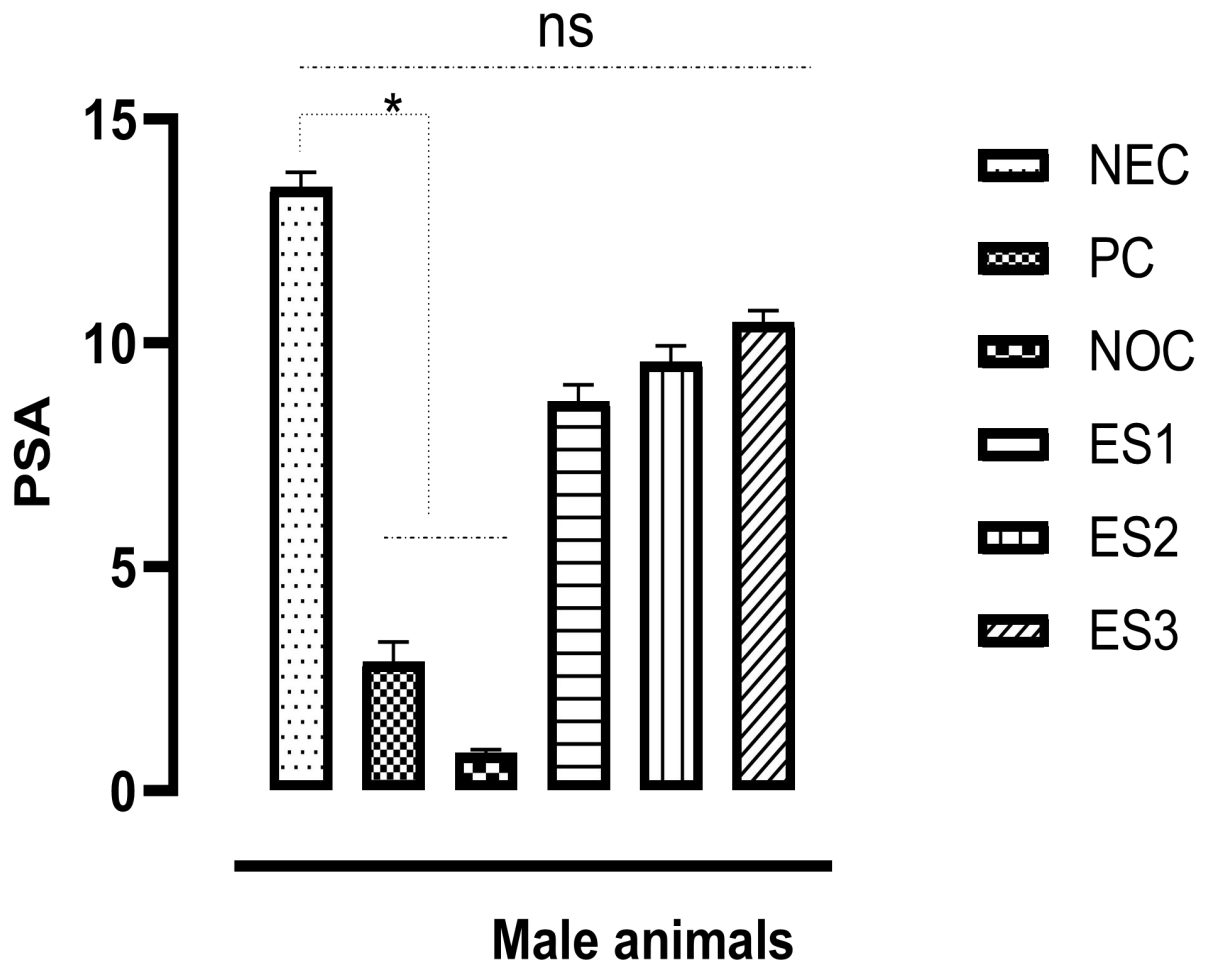
Parameters	B-Mp	S-Mp
The base of Cone (cm)	4.80	6.80
Height of Cone (cm)	1.50	1.80
Angle of Repose (°)	32.00	27.90
Bulk Volume (mL)	9.40	9.60
Tapped Volume (mL)	8.20	9.00
Weight of Powder (g)	6.68	8.88
Bulk Density (g/mL)	0.71	0.93
Tapped Density (g/mL)	0.81	0.99
Compressibility Index (%)	12.35	6.06
Hausner's Ratio	1.14	1.06

Effect of b-mp and s-mp particles on serum psa in BPH-induced male animals

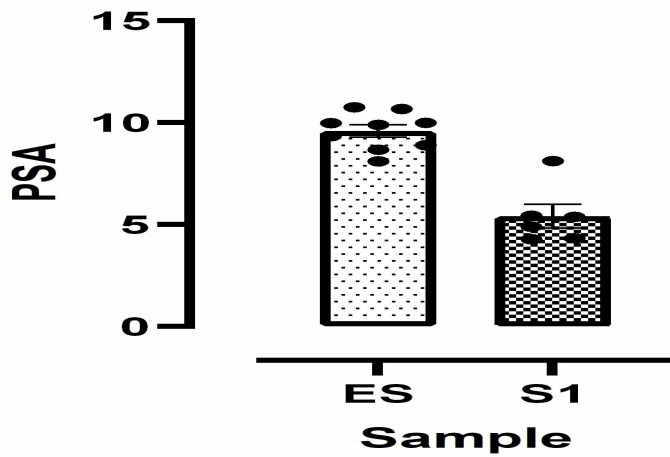
Results from Figure 12A – C, showed that *S. mombin* extract possesses a significant anti-BPH effect in a dose-dependent manner.



A



B



C

A – Effect of different doses of *S. mombin* extract; S1 -3 implies 100, 200, and 400 mg/kg, respectively of *Spondia mombin*)

B – Effect of different doses of microencapsulated *S. mombin* (ES 1 -3 implies 100, 200, and 400 mg/kg respectively of S-Mp while NEC indicates S-Mp)

C – Comparative effect of B-Mp and S-Mp at 400 mg/kg

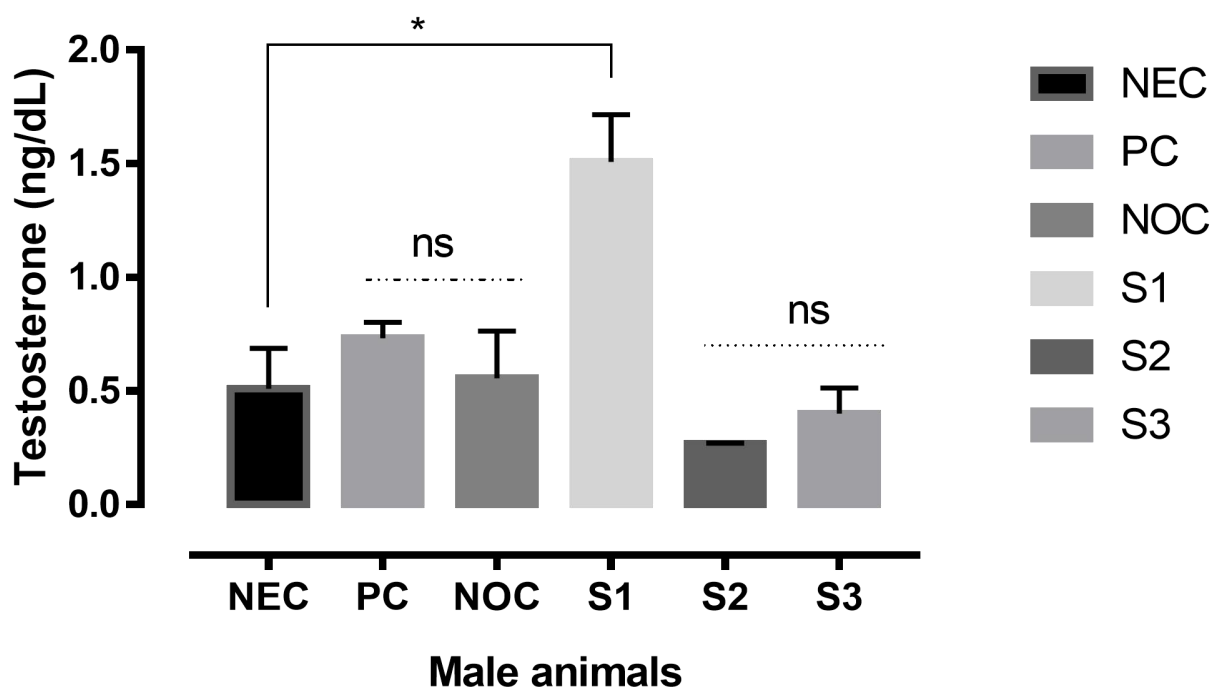
Mean of three replicates. $n=3$. Values with superscripts * indicate a significant difference relative value of negative control $p<0.05$ using Dunnett's test

Figure 12A - C: Influence of *S. mombin*, B-Mp, and S-Mp on serum PSA level in BPH-induced male animals

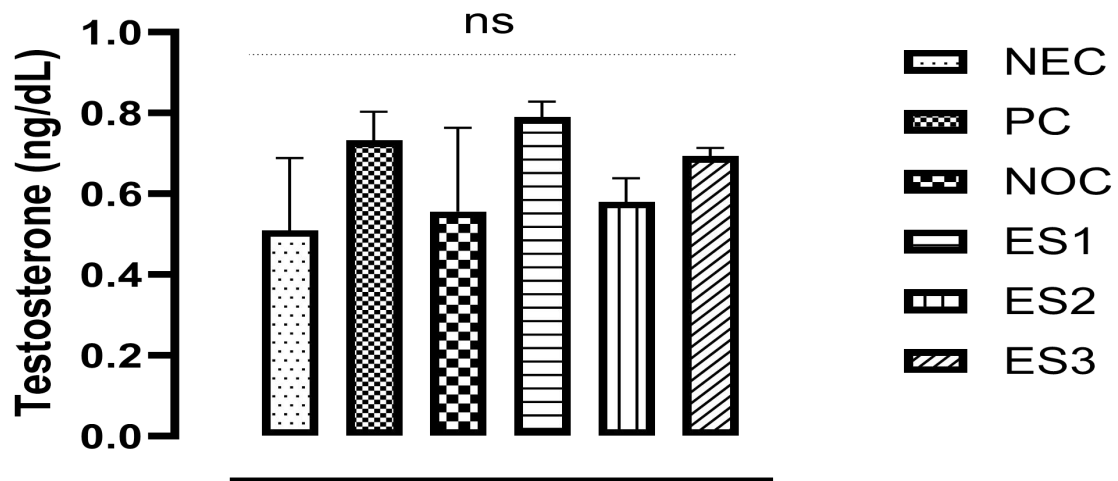
Moreover, the highest amount of PSA (4.82 ng/mL) was observed at 400 mg/kg, which is significantly different at $p<0.05$ from 13.49 ng/mL observed with negative control (B-Mp) as well as 2.51 and 1.79 ng/mL observed with finasteride (positive control) and normal control, respectively as shown in Figure 12A. In addition, a reduction in activity was observed upon encapsulation as shown in Figure 12B. The observed activity of the three doses of ES (also called S-Mp) indicated a high amount of PSA, which is not significant from the values observed with the negative control (B-Mp). Comparative anti-BPH activity at 400 mg/kg of both crude extract of *S. mombin* and microencapsulated particles of *S. mombin* showed a loss in activity which might be due to delayed release of the core (*S. mombin*) from acacia gum matrix, as indicated in Figure 12C.

Effect of samples on serum testosterone in BPH-induced male animals

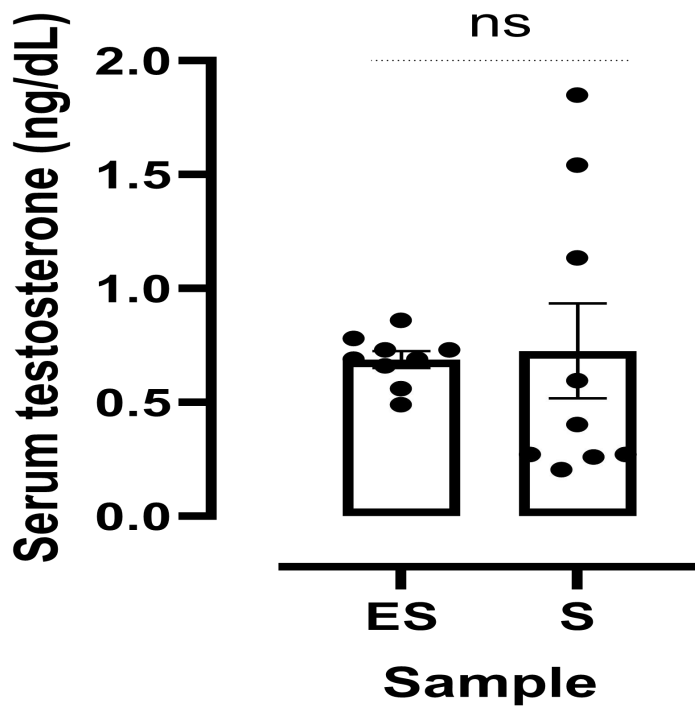
Considering the effect of all the samples on serum testosterone, it was observed that crude extract, blank, and *S. momobin* microencapsulated particles have no significant effect on the serum testosterone level for all the male animals as observed in Figure 13A, B, and C.



A



B



C

A – Effect of different doses of *S. mombin* extract; S1 -3 implies 100, 200, and 400 mg/kg, respectively of *Spondia mombin*)

B – Effect of different doses of microencapsulated *S. mombin* (ES 1 -3 implies 100, 200, and 400 mg/kg respectively of *S-Mp* while NEC indicates *S-Mp*)

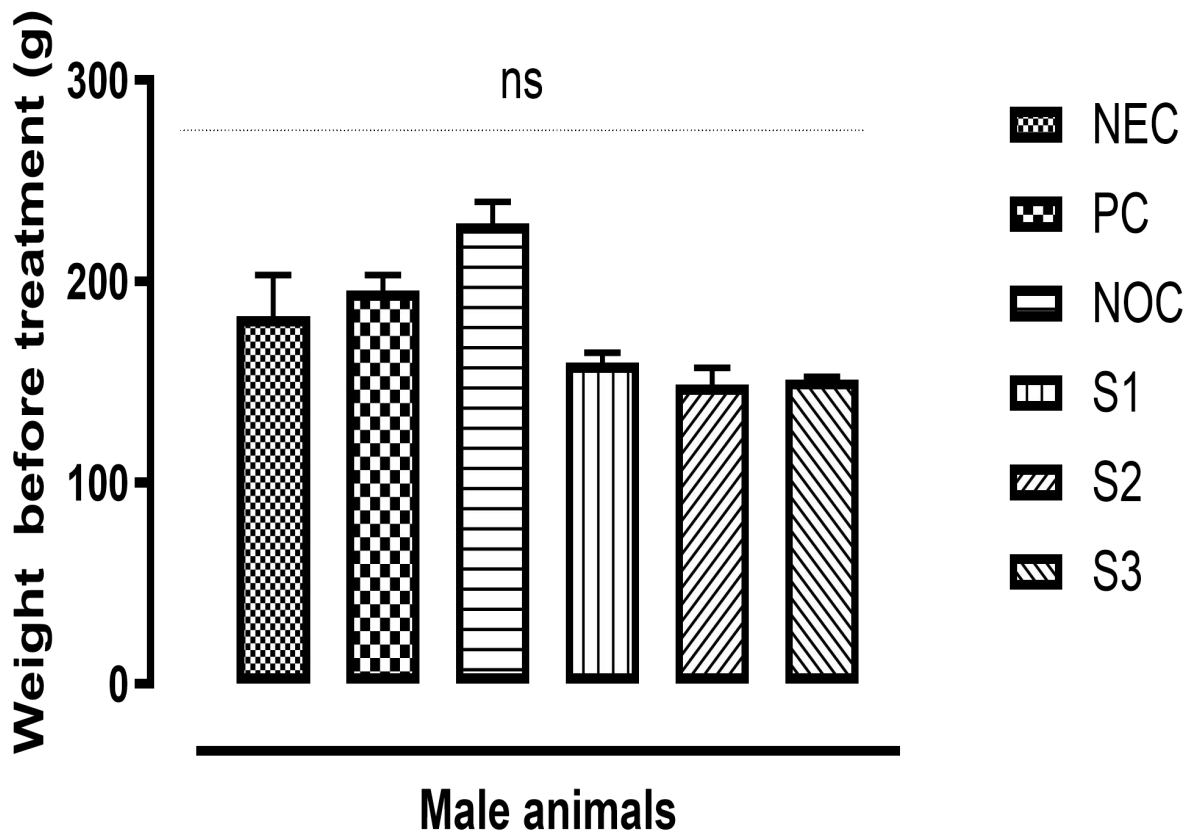
C – Comparative effect of B-Mp and S-Mp at 400 mg/kg

Mean of three replicates. n=3. Values with superscripts * indicate a significant difference relative value of negative control $p < 0.05$ using Dunnett's test

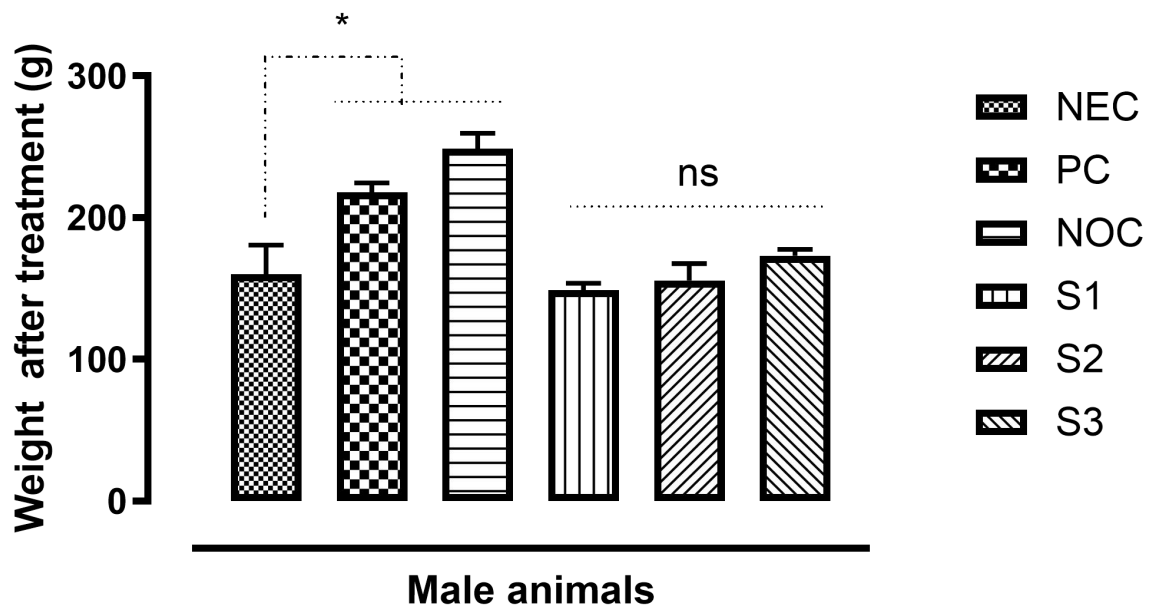
Figure 13A - C: Effect of *S. mombin*, B-Mp, and S-Mp on serum testosterone level in BPH-induced male animals

Effect of samples on animal weights

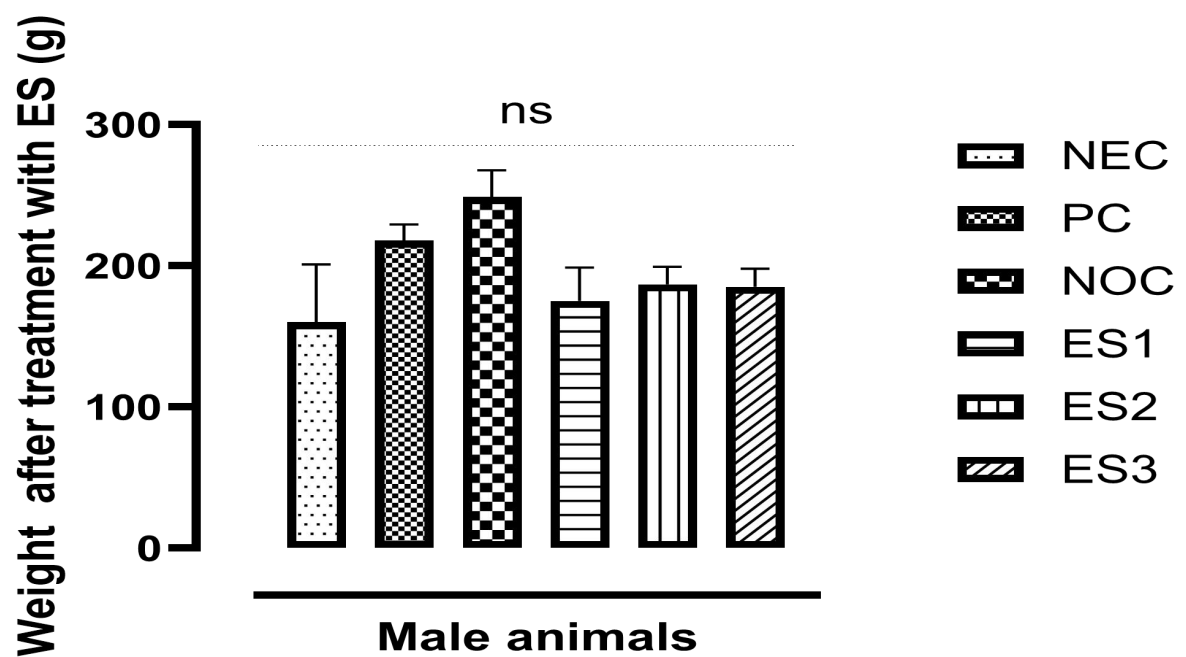
Results obtained from Figure 14A – D showed that the weight of the Wistar rats before and after treatment, there was an increase in weight of the animals administered with *S. mombin* extract, B-Mp, and S-Mp. It is noteworthy to state that, a slight reduction in the weight of the animals administered with B-Mp (negative control) was observed, although the reduction is insignificant as observed in Figures 14A, B, and C. Also, a slight improvement in weight was observed among the animals administered with the crude extract of *S. mombin*, this might explain the reason for the improved promising effect observed in the results of PSA and prostrate index.



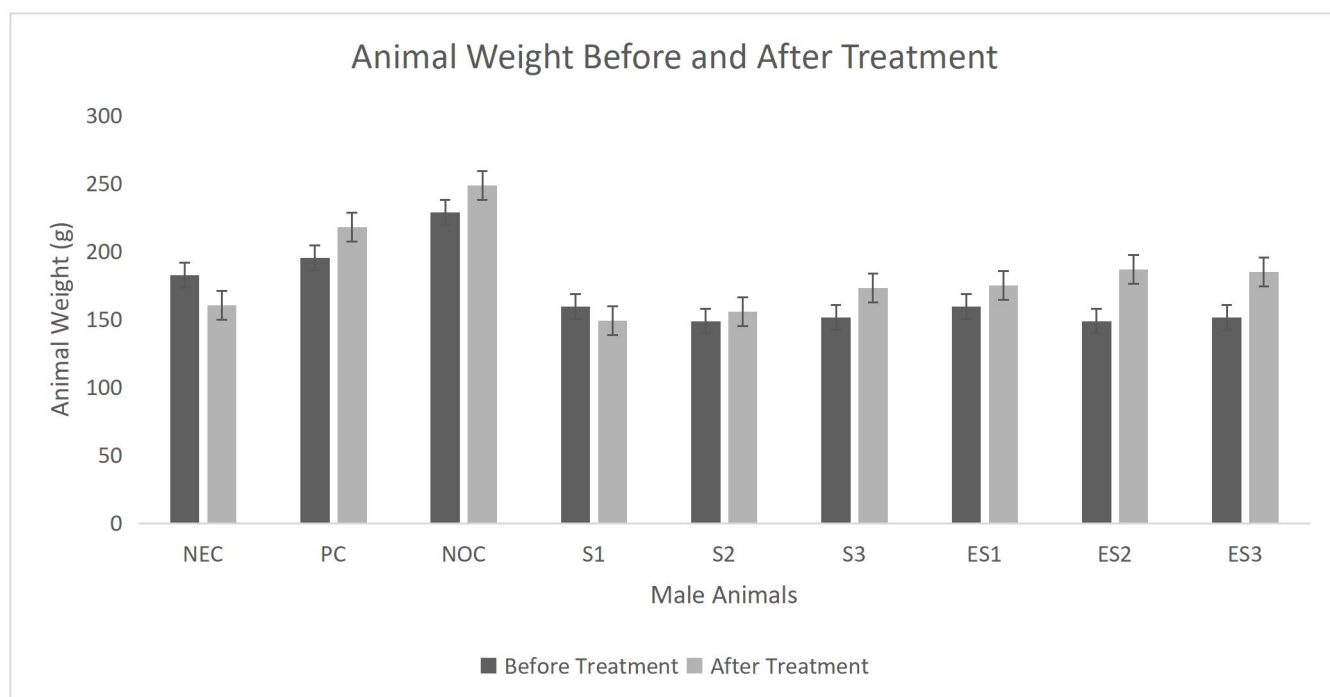
A



B



C

**D**

A – animal weight before treatment with *S. mombin*

B – animal weight after treatment with *S. mombin*

C – animal weight after treatment with microencapsulated *S. mombin* (ES) sample

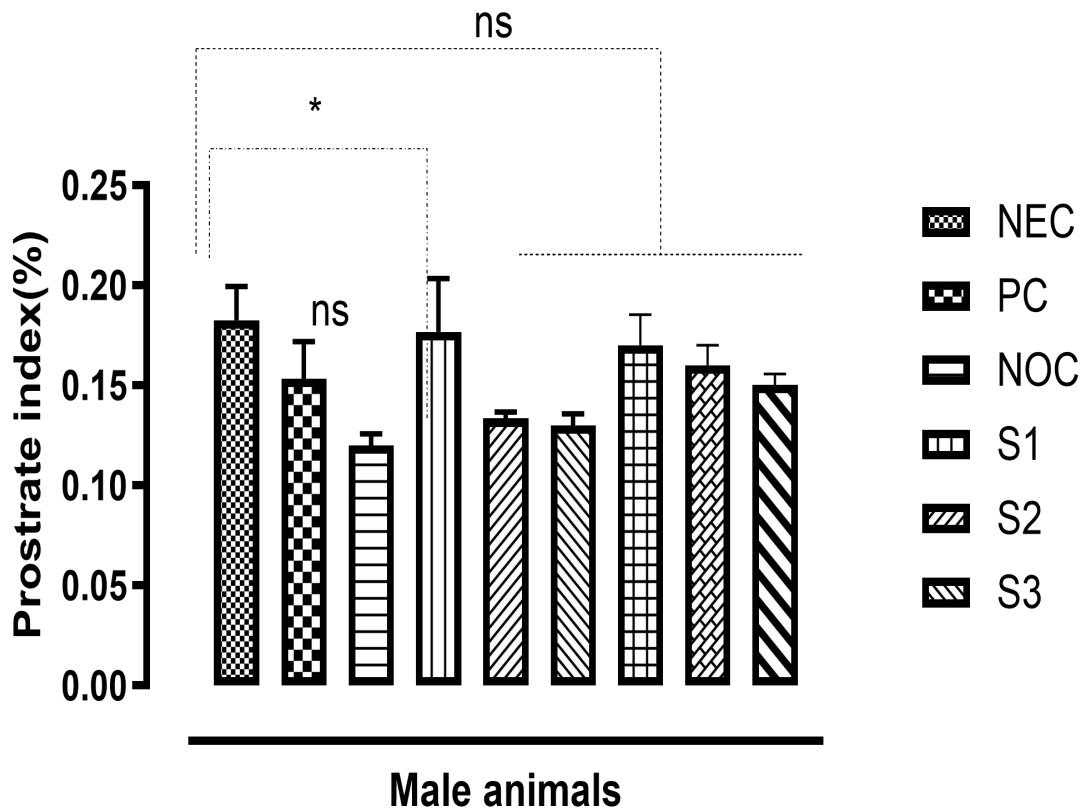
D - relative weight of the male animals before and after treatment with S and ES)

Mean of three replicates. $n=3$. Values with superscripts * indicate a significant difference relative value of negative control $p<0.05$ using Dunnett's test

Figure 14A - D: Animal weight before the induction and after the treatment of testosterone-induced BPH in male animals

Effect of samples on the prostrate index in BPH-induced male animals

The influence of the *S. mombin*, B-Mp, and S-Mp on the prostrate index of animals induced with BPH (Figure 15). The result showed that S-Mp and *S. mombin* induced a reduction in the percentage prostrate index, although the percentage reduction is not significant ($p=0.0630$)



The values above are the mean of three replicates. $n=3$. Values with superscripts * indicate a significant difference relative value of negative control $p<0.05$ using Dunnett's test

Figure 15: Percentage prostrate index of the animal induced with BPH

Dissolution profiles of blank and microencapsulated *Spondia mombin*

Overall, the microencapsulated *Spondia mombin* demonstrated superior dissolution characteristics compared to the blank, as evidenced by the higher absorbance values at all time point (Figure 16).

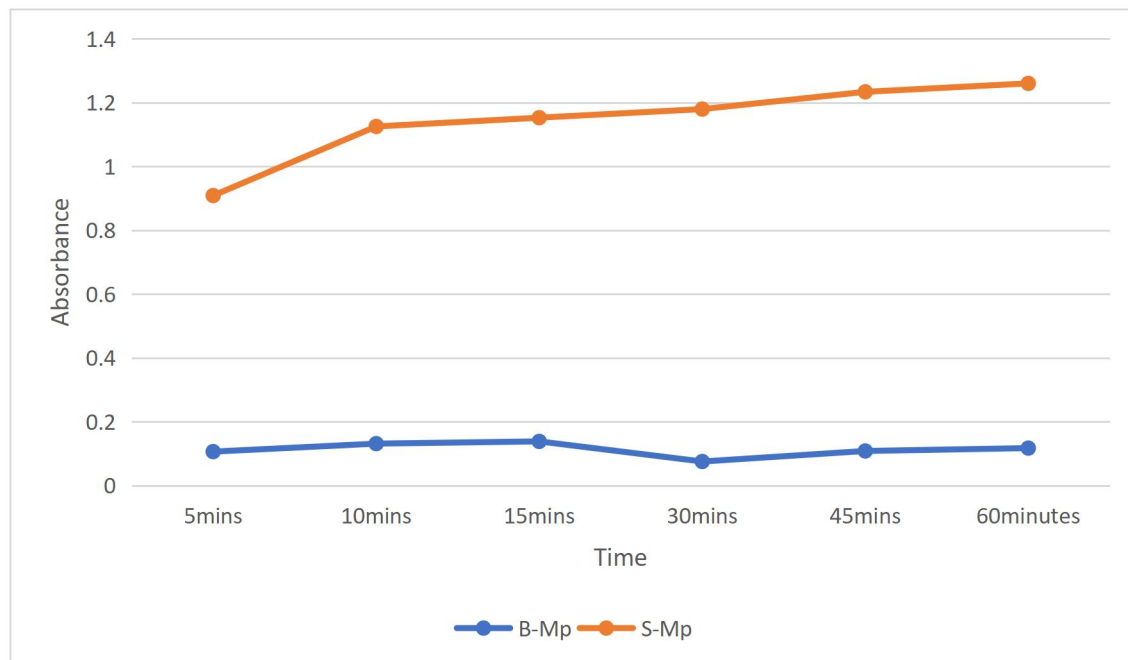


Figure 16. Dissolution Profiles of B-Mp and S-Mp

Discussion

Characterization of microencapsulated *Spondia mombin* l. leaf extract

Microcapsules are known to contribute to the protection of important bioactive (Dias et al., 2015; Sarode et al., 2024). They also possess a wide range of applications in the food industry and pharmaceutical industry (Agnihotri et al., 2012; Sarode et al., 2024).

SEM analysis revealed differences in particle size and morphology between the blank (B-Mp) and microencapsulated (S-Mp) particles, with S-Mp displaying a granular texture and larger size, indicating agglomeration of the active drug, while B-Mp showed smooth, sharp-edged particles. EDX microanalysis highlighted elemental differences, with oxygen being the predominant element in both, showing atomic concentrations of 52.06% to 75.25%, reflecting the organic nature of the materials. Sodium was present in both samples, though in higher concentrations in S-Mp, suggesting its role in the encapsulation matrix. Carbon and sulfur were detected in varying amounts, while calcium was found only in the blank, possibly indicating contamination or a difference in matrix composition between the samples. FTIR analysis of B-Mp and S-Mp revealed similarities and differences. Specific peaks in S-Mp at 1110.7, 1449.9, and 1364.2

wavenumbers were absent in the B-Mp, emphasizing the presence of acacia gum in the blank and highlighting the composition of the active ingredient in the microencapsulated extract. It is noteworthy to state that little or no information has been seen vis a vis SEM analysis of *S. mombin* from previous literature. However Adeyemi et al., (2020) produced a simple non-toxic product of green metallic (Ag, Zn and Cu) nanoparticles using the leaf of *Spondias mombin* and also highlighted that the particles produced exhibited antimicrobial potential.

The angle of repose is a key indicator of powder flowability (Taylor & Aulton, 2021). In this study, the microencapsulated samples B-Mp and S-Mp exhibited angles of repose of 32.00° and 27.90°, respectively. These values suggest that both samples have moderate flow properties, with S-Mp displaying slightly better flowability than B-Mp (Shah et al., 2023). The lower angle of repose in S-Mp indicates reduced interparticle friction, which can be attributed to the differences in particle size, shape, or surface characteristics between the two samples (Shah et al., 2023). The compressibility index and Hausner's ratio are vital parameters for understanding the powder's behaviour under compression. B-Mp exhibited a compressibility index of 12.35%, while S-Mp had a lower

compressibility index of 6.06%. A lower compressibility index typically indicates better flowability and lower susceptibility to caking (Taylor & Aulton, 2021). The corresponding Hausner's ratios were 1.14 for B-Mp and 1.06 for S-Mp, with values closer to 1.00 indicating superior flow properties. These findings suggest that S-Mp is less compressible and has better flowability, making it potentially more suitable for applications requiring precise dosage and consistent performance (Taylor & Aulton, 2021).

The characterization of the microencapsulated *Spondia mombin* L. leaf extract reveals important differences between the two samples, B-Mp and S-Mp, in terms of flowability, density, and compressibility. S-Mp, with its lower angle of repose, higher bulk and tapped densities, lower compressibility index, and more favourable Hausner's ratio, demonstrates superior physical properties compared to B-Mp (Taylor & Aulton, 2021). These characteristics are crucial for the successful formulation of powders intended for oral delivery, where uniformity, ease of handling, and stability are essential (Taylor & Aulton, 2021).

Biological effects of methanolic crude extract and microencapsulated extract of *Spondia mombin* L. in the management of benign prostatic hyperplasia

In addition, the crude extract of *S. mombin* demonstrated a dose-dependent reduction in PSA, with the most significant effect observed at 400 mg/kg. However, S-Mp showed a maximum reduction at 100 mg/kg, with diminishing efficacy at higher doses compared to the crude extract. The crude extract exhibited superior PSA reduction activity than S-Mp. A reduction in serum testosterone was observed upon encapsulation of the crude extract of *S. mombin*, with the most effective decrease observed at 200 mg/kg. Crude extract showed fluctuating testosterone levels at 100 mg/kg, while microencapsulated extract maintained consistent values. The disparity in testosterone levels suggests variations in their physiological effects. Both crude and microencapsulated extracts increased relative animal weight, with the crude extract inducing more weight gain. The varied effects on weight may be attributed to differences in formulation and drug release profiles. Both crude extract of *S. mombin* and S-Mp reduced the percentage prostate index compared to the B-Mp, although no significant difference in the impact was observed among the crude extract, It is noteworthy to state that the variations in

efficacy, especially in PSA reduction, serum testosterone levels, and percentage prostate index, suggest that the encapsulation process significantly influences the bioavailability and pharmacological activity of *S. mombin*, this can be observed via the reduction in activity observed upon encapsulation. This reductive effect might be linked to the delayed release of the plant extract by the acacia gum matrix. Further studies should explore the underlying mechanisms influencing these variations and optimize the microencapsulation techniques for enhanced therapeutic outcomes. However, no experimental data have shown the anti-BPH potential of both crude extract and microencapsulated particles of *S. mombin* based on our findings, but *S. mombin* extracts have been reported to selectively inhibit cell proliferation in the tumour cell line for prostate cancer (PC3) and did not significantly affect healthy cells (Guedes et al., 2020).

The study demonstrates several strengths, particularly in its use of diverse characterization techniques such as Micromeritic evaluation, SEM, EDX, and FTIR analysis, providing a comprehensive understanding of the physical and chemical properties of microencapsulated *Spondia mombin*. This thorough approach enhances the reliability of the findings. The biological relevance of the research is also a major

strength, as it investigates the effects of crude and microencapsulated *S. mombin* on BPH-induced male animals, assessing parameters like PSA reduction, serum testosterone, and prostate index. Additionally, the dose-dependent analysis provides valuable insights into the optimal dosage for therapeutic efficacy, making the study more applicable to clinical settings.

The study contributes significantly to the knowledge of *S. mombin*'s therapeutic potential, particularly its anti-BPH effects. It offers new insights into how microencapsulation with acacia gum affects the release profile and efficacy of *S. mombin*'s bioactive compounds, providing a basis for optimizing drug delivery systems. Comparative pharmacological analysis between crude and microencapsulated forms furthers understanding of their physiological effects, particularly in PSA reduction and prostate health. The research highlights the need for optimization in microencapsulation techniques, directing future studies towards improving the bioavailability and efficacy of *S. mombin* extracts.

Dissolution study of microencapsulated *Spondia mombin* l. leaf extract

The dissolution study results indicate that the microencapsulation of *Spondia mombin* significantly improves its dissolution profile compared to the blank microencapsulated

formulation. The higher absorbance values for the *Spondia mombin* extract suggest enhanced solubility and possibly better bioavailability, which can be attributed to the microencapsulation process (Chen et al., 2019). Microencapsulation is known to improve dissolution rates by reducing particle size, increasing surface area, and enhancing the interaction of the active ingredient with the dissolution medium (Jyothi et al., 2010; Kuang et al., 2010). In this study, *Spondia mombin* demonstrated a steady increase in absorbance over time, indicating a sustained and gradual release of the active components. This is particularly important for formulations that require controlled or extended release, as the gradual increase in absorbance reflects the efficient release of the encapsulated compound. By 60 minutes, the absorbance for *Spondia mombin* extract reached its peak (1.2600), indicating that the microencapsulation process was effective in enhancing dissolution, possibly due to improved wettability or interaction with the dissolution medium. This finding is consistent with other studies that show microencapsulation can lead to improved dissolution rates, particularly for poorly soluble compounds (Khadka et al., 2014; Molina et al., 2022).

Conclusions

The field of herbal medicine is advancing through the standardization and modification of herbal extracts, alongside innovations like microencapsulation, which enhances stability, bioavailability, and controlled drug release. This study demonstrates that *S. mombin* has significant anti-BPH activity, supporting its traditional use in prostate health. However, encapsulation with acacia gum reduced the extract's efficacy, suggesting a need to optimize the process for improved bioavailability. Future research should focus on refining microencapsulation techniques, evaluating the drug release profiles, and comparing encapsulating agents to maximize therapeutic potential. Long-term studies are essential to assess the safety and efficacy of both crude and encapsulated forms of *S. mombin*.

Acknowledgements: We the authors sincerely appreciate the management and staff of Afe Babalola University, Igbinedion University, and Igbinedion College of Health Technology, Nigeria for the assistance rendered during this research. A special appreciation to Dr. Samuel Odewo (taxonomist from the Forestry Research Institute of Nigeria), who suggested the name of the plant used for this research.

Conflict of interest: The authors declare no conflict of interest

Author's contributions: IAK, ND, AO and KI: Conceptualization, Funding acquisition, Project administration, Supervision, Writing—review & editing; IAK, ND, AO and KI: Methodology, Formal analysis, Software, Writing—review & editing,

Funding acquisition; IAK, ND, AO and KI: Data curation, Formal analysis, Investigation, Writing—original draft; AO: Investigation, Validation; IAK, ND, AO and KI: Writing—review & editing.

Funding: We the authors provided funding for this research

References

- Adeniran, A. A., Ntamanwuna, E. C., & Bassey, V. O. (2021). Microscopical characterization and physicochemical standardization of leaves, stems and roots of *Spondias mombin* L.(Anacardiaceae). *Nigerian Journal of Pharmaceutical Research*, 17(1), 15–25.
- Adepu, S., & Ramakrishna, S. (2021). Controlled drug delivery systems: Current status and future directions. *Molecules*, 26(19), 5905.
- Adeyemi, D. K., Adeluola, A. O., Akinbile, M. J., Johnson, O. O., & Ayoola, G. A. (2020). Green synthesis of Ag, Zn and Cu nanoparticles from aqueous extract of *Spondias mombin* leaves and evaluation of their antibacterial activity. *African Journal of Clinical and Experimental Microbiology*, 21(2), 106–113.
- Agnihotri, N., Mishra, R., Goda, C., & Arora, M. (2012). *Microencapsulation – A Novel Approach in Drug Delivery: A Review*.
- Aiyelaja, A. A., & Bello, O. A. (2006). Ethnobotanical potentials of common herbs in Nigeria: A case study of Enugu state. *Educational Research and Reviews*, 1(1), 16.
- Alamgir, A. N. M., & Alamgir, A. N. M. (2017). Herbal drugs: Their collection, preservation, and preparation; evaluation, quality control, and standardization of herbal drugs. *Therapeutic Use of Medicinal Plants and Their Extracts: Volume 1: Pharmacognosy*, 453–495.
- Aromolaran, O., & Badejo, O. K. (2014). Efficacy of fresh leaf extracts of *Spondias mombin* against some clinical bacterial isolates from typhoid patients. *Asian Pacific Journal of Tropical Disease*, 4(6), 442–446.

- Asante Ampadu, G. A., Mensah, J. O., Darko, G., & Borquaye, L. S. (2022). Essential oils from the fruits and leaves of *Spondias mombin* linn.: Chemical composition, biological activity, and molecular docking study. *Evidence-Based Complementary and Alternative Medicine*, 2022.
- Chen, L., Gnanaraj, C., Arulselvan, P., El-Seedi, H., & Teng, H. (2019). A review on advanced microencapsulation technology to enhance bioavailability of phenolic compounds: Based on its activity in the treatment of Type 2 Diabetes. *Trends in Food Science & Technology*, 85, 149–162. <https://doi.org/10.1016/j.tifs.2018.11.026>
- Dias, M. I., Ferreira, I. C., & Barreiro, M. F. (2015). Microencapsulation of bioactives for food applications. *Food & Function*, 6(4), 1035–1052.
- George, T. T., Oyenih, A. B., Rautenbach, F., & Obilana, A. O. (2021). Characterization of *Moringa oleifera* leaf powder extract encapsulated in maltodextrin and/or gum arabic coatings. *Foods*, 10(12), 3044.
- Guedes, J. A. C., Alves Filho, E. G., Silva, M. F. S., Rodrigues, T. H. S., Ramires, C. M. C., Lima, M. A. C., Silva, G. S., Pessoa, C. Ó., Canuto, K. M., Brito, E. S., Alves, R. E., Nascimento, R. F., & Zocolo, G. J. (2020). GC-MS-Based Metabolomic Profiles Combined with Chemometric Tools and Cytotoxic Activities of Non-Polar Leaf Extracts of *Spondias mombin* L. and *Spondias tuberosa* Arr. Cam. *Journal of the Brazilian Chemical Society*, 31, 331–340. <https://doi.org/10.21577/0103-5053.20190185>
- Iwu, I. C., Alisa, C., Anukam, B., Bilar, A., Ezekoye, M. O., Igbomezie, M. C., Anozie, R. C., Okoro, M. U., & Obiagwu, I. (2022). Chemical and Medicinal Properties of *Spondias Mombim* (Linn) Leaf Harvested from The South Eastern Nigeria. *Global Journal of Pure and Applied Chemistry Research*, 10(1), 1–22.
- Jayanudin, Fahrurrozi, M., Wirawan, S. K., & Rochmadi. (2019). Preparation of chitosan microcapsules containing red ginger oleoresin using emulsion crosslinking method. *Journal of Applied Biomaterials & Functional Materials*, 17(1), 2280800018809917.
- Jyothi, N. V. N., Prasanna, P. M., Sakarkar, S. N., Prabha, K. S., Ramaiah, P. S., & Srawan, G. Y. (2010). Microencapsulation techniques, factors influencing encapsulation efficiency. *Journal of Microencapsulation*, 27(3), 187–197.

<https://doi.org/10.3109/0265204090313130>

1

Khadka, P., Ro, J., Kim, H., Kim, I., Kim, J. T., Kim, H., Cho, J. M., Yun, G., & Lee, J. (2014). Pharmaceutical particle

technologies: An approach to improve drug solubility, dissolution and bioavailability.

Asian Journal of Pharmaceutical Sciences, 9(6), 304–316.

<https://doi.org/10.1016/j.ajps.2014.05.005>

Kim, E. H., Brockman, J. A., & Andriole, G.

L. (2018). The use of 5-alpha reductase inhibitors in the treatment of benign

prostatic hyperplasia. *Asian Journal of Urology*, 5(1), 28–32.

Kim, E. H., Larson, J. A., & Andriole, G. L.

(2016). Management of Benign Prostatic Hyperplasia. *Annual Review of Medicine*, 67(1), 137–151.

<https://doi.org/10.1146/annurev-med-063014-123902>

Kuang, S. S., Oliveira, J. C., & Crean, A. M.

(2010). Microencapsulation as a Tool for Incorporating Bioactive Ingredients into Food. *Critical Reviews in Food Science and Nutrition*, 50(10), 951–968.

<https://doi.org/10.1080/1040839090304422>

2

Lam, P. L., & Gambari, R. (2014).

Advanced progress of microencapsulation technologies: In vivo and in vitro models for studying oral and transdermal drug deliveries. *Journal of Controlled Release*, 178, 25–45.

Lee, S. W. H., Chan, E. M. C., & Lai, Y. K.

(2017). The global burden of lower urinary tract symptoms suggestive of benign prostatic hyperplasia: A systematic review and meta-analysis. *Scientific Reports*, 7(1), 7984.

Lengyel, M., Kállai-Szabó, N., Antal, V., Laki, A. J., & Antal, I. (2019).

Microparticles, microspheres, and microcapsules for advanced drug delivery. *Scientia Pharmaceutica*, 87(3), 20.

Lepor, H. (2016). Alpha-blockers for the treatment of benign prostatic hyperplasia. *Urologic Clinics*, 43(3), 311–323.

Li, J., Tian, Y., Guo, S., Gu, H., Yuan, Q., & Xie, X. (2018). Testosterone-induced benign prostatic hyperplasia rat and dog as facile models to assess drugs targeting lower urinary tract symptoms. *PLoS ONE*, 13(1), e0191469.

<https://doi.org/10.1371/journal.pone.0191469>

9

- Liu, D., Kottke, I., & Adam, D. (2007). Localization of cadmium in the root cells of *Allium cepa* by energy dispersive X-ray analysis. *Biologia Plantarum*, 51, 363–366.
- Lopez-Mendez, T. B., Santos-Vizcaino, E., Pedraz, J. L., Orive, G., & Hernandez, R. M. (2021). Cell microencapsulation technologies for sustained drug delivery: Latest advances in efficacy and biosafety. *Journal of Controlled Release*, 335, 619–636.
- Molina, V., von Plessing, C., Romero, A., Benavides, S., Troncoso, J. M., Pérez-Correa, J. R., & Franco, W. (2022). Determination of the Dissolution/Permeation and Apparent Solubility for Microencapsulated Emamectin Benzoate Using In Vitro and Ex Vivo *Salmo salar* Intestine Membranes. *Pharmaceuticals*, 15(6), 652. <https://doi.org/10.3390/ph15060652>
- Nworu, C. S., Akah, P. A., Okoye, F. B., Toukam, D. K., Udeh, J., & Esimone, C. O. (2011). The leaf extract of *Spondias mombin* L. displays an anti-inflammatory effect and suppresses inducible formation of tumor necrosis factor- α and nitric oxide (NO). *Journal of Immunotoxicology*, 8(1), 10–16.
- Ogunro, O. B., Oyeyinka, B. O., Gyebi, G. A., & Batiha, G. E.-S. (2023). Nutritional benefits, ethnomedicinal uses, phytochemistry, pharmacological properties and toxicity of *Spondias mombin* Linn: A comprehensive review. *Journal of Pharmacy and Pharmacology*, 75(2), 162–226. <https://doi.org/10.1093/jpp/rgac086>
- Osuntokun, O. T. (2018). Evaluation of Inhibitory Zone Diameter (IZD) of crude *Spondias mombin* (Linn.) extracts (root, leaf, and stem bark) against thirty infectious clinical and environmental isolates. *J Bacteriol Infec Dis*. 2018; 2 (1): 8, 16.
- Osuntokun, O. T. (2019). *Exploring the Medicinal Efficacy, Properties and Therapeutic uses of Spondias mombin (Linn)* *Int J Appl Res Med Plants* 2: 115.
- Parasuraman, S., Raveendran, R., & Kesavan, R. (2010). Blood sample collection in small laboratory animals. *Journal of Pharmacology & Pharmacotherapeutics*, 1(2), 87–93. <https://doi.org/10.4103/0976-500X.72350>
- Rani, S., & Goel, A. (2021). Microencapsulation technology in textiles: A review study. *Pharma Innov J*, 10, 660–663.

- Sangeetha, B., Krishnamoorthy, A. S., Amirtham, D., Sharmila, D. J. S., Renukadevi, P., & Malathi, V. G. (2019). FT-IR spectroscopic characteristics of *Ganoderma lucidum* secondary metabolites. *J. Appl. Sci. Technol*, 38, 1–8.
- Sarode, S. A., Sarode, M. A., Sonawane, Y. N., Patil, P. R., Thakare, A. U., Somwanshi, T. V., & Suralkar, R. K. (2024). Microencapsulation Technology For Novel Pharmaceutical Formulations. *International Journal of Pharmaceutical Sciences*, 2(02), 1–1.
- Shah, D. S., Moravkar, K. K., Jha, D. K., Lonkar, V., Amin, P. D., & Chalikwar, S. S. (2023). A concise summary of powder processing methodologies for flow enhancement. *Heliyon*, 9(6).
<https://doi.org/10.1016/j.heliyon.2023.e16498>
- Singh, H., Gauri. (2023). Recent development of novel drug delivery of herbal drugs. *RPS Pharmacy and Pharmacology Reports*, 2(4), rqad028.
<https://doi.org/10.1093/rpsppr/rqad028>
- Singh, M. N., Hemant, K. S. Y., Ram, M., & Shivakumar, H. G. (2010). Microencapsulation: A promising technique for controlled drug delivery. *Research in Pharmaceutical Sciences*, 5(2), 65–77.
- Smith, K. M., & Xu, Y. (2012). Tissue sample preparation in bioanalytical assays. *Bioanalysis*, 4(6), 741–749.
- Taylor, K. M. G., & Aulton, M. E. (2021). *Aulton's Pharmaceutics E-Book: Aulton's Pharmaceutics E-Book*. Elsevier Health Sciences.
- Thilagavathi, G., Bala, S. K., & Kannaian, T. (2007). Microencapsulation of herbal extracts for microbial resistance in healthcare textiles. *INDIAN J. FIBRE TEXT. RES.*
- Xiong, Y., Zhang, Y., Li, X., Qin, F., & Yuan, J. (2020). The prevalence and associated factors of lower urinary tract symptoms suggestive of benign prostatic hyperplasia in aging males. *The Aging Male*, 23(5), 1432–1439.